Research on Engineering Structures & Materials
www.jresm.org
Research Group

Research Article

Comparative investigation of dynamic resilience and vibration characteristics of one-way concrete slabs reinforced with steel bars, GFRP bars and steel wire ropes

Ahmed Mohammed Ahmed [*,1,a], Aziz Ibrahim Abdulla [2,b]

[1]*Department of Civil Engineering, University of Samarra, College of Engineering, Iraq*
[2]*Department of Civil Engineering, Tikrit University, College of Engineering, Iraq*

Article Info

Article History:

Received 05 July 2026
Accepted 03 Aug 2026

Keywords:

Dynamic response;
GFRP bars;
Steel wire rope;
Steel alternatives;
Bar diameter;
Damping ratio;
Natural frequency

Abstract

The effect of reinforcement material type and bar diameter on the dynamic response of one-way slab panels is studied in this research work. The experimental program included testing twelve one-way, simply supported slab panels under a low-velocity impact through a 10 kg mass freely falling from a height of 1 m. Three systems of reinforcement were considered: deformed steel bars, GFRP bars, and steel wire ropes. Four specimens were cast for each type of reinforcement, each specimen was reinforced with one of four diameters (6, 8, 12, and 16 mm). Under dynamic excitation, the three-reinforcement series exhibited distinctly different vibration characteristics, with damping ratios, natural frequencies, and peak amplitudes varying in a manner directly related to the stiffness of each reinforcement type. The lowest midspan amplitude values and the highest natural frequency (18.5–16.67 Hz) were achieved by steel-reinforced panels; therefore, it is recommended to use deformed steel bars in reinforcing members when lower vibration amplitude is required. Panels reinforced by 12 mm diameter GFRP bars (G-12) recorded the highest damping ratio (12.5%), meaning that the vibration diminished faster than any other among the twelve specimens. This behavior affirms that reinforcement selection governs not only static load-carrying behavior but also the dynamic resilience of the structural element.

1. Introduction

In some specific conditions, traditional steel bars could be replaced by fiber-reinforced polymer bars [1]. In concrete members exposed to high levels of chloride [2] or bridge slabs where the use of deicing salts promotes the rapid corrosion of steel reinforcement [3,4]. It is recommended to use composite reinforcing bars due to their resistance to aggressive environments. Extensive research has been conducted in the field of reinforcement alternatives and their use in concrete elements. Below are some of the research efforts focused on the behavior of reinforced concrete elements reinforced by steel and steel alternatives under dynamic loading conditions.

According to Liu and Zou, dynamic energy dissipation can be significantly enhanced without compromising stiffness when reinforcement and transverse detailing are properly chosen. For members, the damping ratio increases with GFRP ratio up to an optimum of about 0.9 %, then decreases as section rigidity dominates. Closely spaced stirrups further increase damping. Pull-out tests indicate that average bond stress improved with smaller bar diameter, shorter embedment, thicker concrete cover and ribbed rather than smooth surface [5]. Concrete slabs reinforced with steel and GFRP bars were tested using a 105 kg conical impactor dropped from 2.5 m and responses were recorded via LVDTs, strain gauges and accelerometers. GFRP reinforced slabs generally

*Corresponding author: ahmed_m@uosamarra.edu.iq
[a]orcid.org/0000-0001-7519-7053; [b]orcid.org/0000-0002-1909-2350;
DOI: http://dx.doi.org/10.17515/resm2026-1821ma0705rs

showed larger displacements and more cracking but could match or outperform steel reinforced slabs when a higher GFRP ratio was provided [6].

FRP primarily limits crack width and concrete damage by remaining elastic, whereas steel governs energy dissipation; consequently, the FRP-steel volume ratio controls both residual deformation and absorbed impact energy, with an optimal balanced configuration at approximately 50% FRP. Hybrid slabs exhibited more distributed, partially recoverable cracking than regular slabs. Although over-reinforcement is effective in limiting deflection, it is discouraged as it diminishes energy absorption and may increase damage demand on concrete [7]. In full-scale one-way concrete slabs reinforced either with GFRP bars of conventional steel, strains are highest along the short span and near the impact point, confirming that flexural response is governed by the primary spanning direction under local impact. GFRP-reinforced slabs exhibit lower maximum strains and significantly shorter strain-decay time with pulse suppression time lower than steel-reinforced slabs at the same impact height, indicating improved impact resistance and faster dynamic recovery despite similar concrete mixes [8].

UHPC/SFR-UHPC slabs with 8 mm CFRP tension bars achieved similar or slightly lower peak displacements than their steel reinforced counterparts but exhibit notably smaller crack widths, limited scabbing, and superior impact damage resistance since neither CFRP nor steel yields in high strength concretes. Normal-strength concrete control slab fails through severe localized punching-shear, diagonal cracking, bond deterioration, bar yielding and concrete perforation beneath the impactor. Using equivalent area of CFRP bars of smaller diameter 4.66 mm in normal strength concrete increases the slab maximum displacement with widened diagonal cracks on the tension zone. Slab impact resistance is governed primarily by concrete compressive and shear strength rather than reinforcement strength [9]. Stainless steel wire reinforcement markedly enhanced impact toughness and suppressed crack propagation through the formation of inter-anchored among bundled wires. Notably, however, the addition of stainless-steel wire attenuated the inherent strain-rate strengthening effect of a plain reactive powder concrete [10].

The three-dimensional micron-diameter wire network effectively suppressed crack initiation and propagation, with dynamic impact toughness and energy dissipation increased by 43.5% and 58.2%, respectively, relative to ordinary concrete at 1.5% volume wire content. Slab thickness is the most influential parameter governing maximum deflection, followed by scaled distance, reinforcement ratio and slab length. Increasing thickness from 40 to 90mm reduced deflection by 82% [11]. Stainless steel wire-reinforced UHPC door panels substantially outperformed normal concrete, HPC and SFR-UHPC, reducing spalling damage and fragment ejection under close-range explosions. At merely 62.5% of conventional panel thickness, stainless steel wire-reinforced UHPC offered 2.9 times greater projectile impact resistance at 600 m/s [12].

According to ACI code, detailing of steel reinforcement is important to control cracking. Many fine cracks are preferable to a few wide cracks for better durability and appearance. Spacing of reinforcement and concrete cover were found to be significant variables reflecting detailing of the reinforcement. Well-distribution of reinforcement in the maximum tension zone helps in controlling cracking. For that, several bars at moderate spacing are much more effective in controlling cracking than one or two large bars of equivalent area [13]. Theoretically, changing reinforcement bar diameter affects the cumulative bond parameter per unit length, specific shear bond stress per unit contact area and distribution of reinforcement. Specimens reinforced with smaller-diameter bars possess substantially larger cumulative bond parameter per unit length, generating more extensive micro-frictional interaction at the steel-concrete interface. Assessing how the reinforcement configuration affects the behavior of concrete structures is important in making the right decision in the design of concrete members. This project aims to understand the impact of changing reinforcement bar diameters on the behavior of one-way slab panels reinforced by steel alternatives and compared with panels reinforced by traditional steel. An experimental program is applied casting several slab panels, changing reinforcement type and bar diameter and assessing their behavior under dynamic loading conditions.

2. Experimental Program

The experimental program included casting 12 reinforced concrete slab panels with dimensions. 4000×1000×180 mm. The panels were tested under dynamic impulse and measuring the dynamic response due to low velocity dropped object [9, 14, 15]. Slab panels were reinforced by three different types of reinforcement individually and every panel was reinforced by different reinforcement diameter with the same reinforcement ratio for the specimens of every series as shown in the table below.

Table 1. Specimen reinforcement details

symbol	No of bars	Reinforcement area	description
S-6	20 Φ 6	565.48	Slab panel reinforced by 6 mm diameter steel bars
S-8	12 Φ 8	603.19	Slab panel reinforced by 8 mm diameter steel bars
S-12	5 Φ 12	565.48	Slab panel reinforced by 12 mm diameter steel bars
S-16	3 Φ 16	603.19	Slab panel reinforced by 16 mm diameter steel bars
G-6	20 Φ 6	565.48	Slab panel reinforced by 6 mm diameter GFRP bars
G-8	12 Φ 8	603.19	Slab panel reinforced by 8 mm diameter GFRP bars
G-12	5 Φ 12	565.48	Slab panel reinforced by 12 mm diameter GFRP bars
G-16	3 Φ 16	603.19	Slab panel reinforced by 16 mm diameter GFRP bars
W-6	20 Φ 6	372.655	Slab panel reinforced by 6 mm diameter steel wire rope
W-8	12 Φ 8	397.45	Slab panel reinforced by 8 mm diameter steel wire rope
W-12	5 Φ 12	373.25	Slab panel reinforced by 12 mm diameter steel wire rope
W-16	3 Φ 16	397.45	Slab panel reinforced by 16 mm diameter steel wire rope

Note: The gross cross-sectional area of wire rope reinforcement is lower than steel and GFRP counterparts due to the 65% fill factor of wire ropes.

Note: Only a single specimen for each configuration was cast and tested, it is recommended to test multiple specimens to improve statistical reliability in future studies.

2.1. Material

The same ready-mixed concrete was used in casting all slabs in this research at the same time and under the same conditions. To achieve this a ready mixed concrete truck with capacity of ten cubic meters was delivered to the worksite to cast the twelve slabs together at one time. Concrete targeted compressive strength was 25.2 MPa. Three concrete cylindrical samples were taken from the truck to test the compressive strength according to [16].

Table 2. Concrete mix mechanical properties

Type	Compressive strength (MPa)	Tensile strength (MPa)	Modulus of rupture (MPa)
C 25	25.2	2.83	2.61

The control specimens were reinforced by traditional deformed steel bars matching ASTM A615 [17]. Four slab panels were reinforced by deformed steel bars with different bar diameters for each panel maintaining the same reinforcement ratio (the number of bars will be different). Four specimens were reinforced by ribbed GFRP bars using four different bar diameters. Every single slab was reinforced by different bar diameters maintaining the same area of reinforcement. Table 3 presents the mechanical characteristics of GFRP bas provided by the manufacturer who tested specimens according to ISO10406 (FRP reinforcement of concrete. Test methods) [17]. Steel wire ropes with four wire diameters were used in four slab specimens. Every slab was reinforced with one different diameter provided that the steel area is fixed (the number of wires will be different). The type used in this study is the (7x19) IWRC. Table 4 presents the mechanical characteristics of deformed steel bars and steel wire ropes tested in Tikrit University mechanical laboratories according to ASTM A615 and ASTM A931 respectively. [18], [19].

Table 3. GFRP bars mechanical properties

Reinforcement	Ultimate Tensile Strength (MPa)	Modulus of Elasticity (MPa)
G-6	1300	51125
G-8	1840	72521
G-12	1331	51197
G-16	1204	52725

Table 4. Steel bars and wire ropes mechanical properties

Reinforcement	Yield Strength (MPa)	Ultimate strength (MPa)	Elongation %	Modulus of Elasticity (MPa)
S-6	407	491	4.8	185000
S-8	422	552	6.5	215350
S-12	430	608	14.2	193650
S-16	626	740	15.4	207150
W-6	350.62	561.1	3.71	102000
W-8	351.05	437.36	5.7	105500
W-12	361.2	535.7	6.13	100180
W-16	345.24	350	6.22	108250

2.2. Stages of Work

2.2.1 Preparation of The Specimens

The panels were cast on two parallel supporting walls built for this purpose with 3600 mm clear distance between them. Specimens were cast using the same concrete mixture with 25.2 MPa compressive strength.

Fig. 1. Supporting walls

Fig. 2. Panels formwork

2.2.2 Dynamic Test

The dynamic test involved evaluating the dynamic response of the slabs through a 10 kg metal mass (ball) freely dropped - from a height of 1 m to the midspan of the panel and recording the resulting response. The mass dropped without any guideway to eliminate any effect of friction losses. After the drop, the vibration amplitude and acceleration at midspan were measured as shown in figure 3. The accelerometer sensor used was (GY-61 ADXL335 3-axis) and the LVDT used was (SOPG20). The dynamic LVDT end was firmly connected to the bottom of the panel to ensure compatible vibration characteristics as shown in figure 4. The amount of the falling mass (10 kg) and the height (1 m) is chosen to ensure no cracks were propagated in the panel due to the impact. However; this goal was verified through an Ultrasonic pulse velocity test on the bottom face of the panel, which showed no significant variation in pulse velocity was recorded before and after the impact was applied, which confirmed that no cracks were propagated due to the impact.

Table 5. LVDT sensor specification

Reinforcement	Specification
Supply voltage	9-12VDC
Operating current	≤12mA
Measuring range	50mm, 100mm
Output signal	0-5v
Linearity	0.25%, 0.5%
Stok length	50mm, 100mm
Resolution	≤0.1um, 16bit

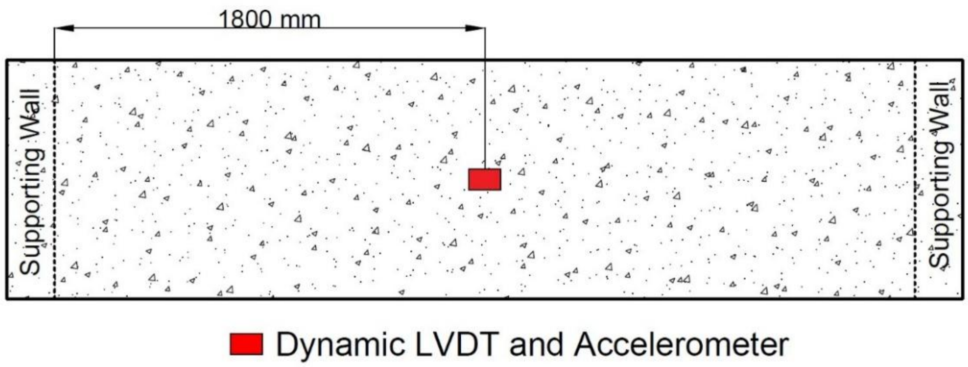

Fig. 3. Position of LVDT

Fig. 4. Dynamic LVDT and accelerometer

3. Results and Discussion

The dynamic response of reinforced concrete slab panels under transient impact excitation is governed by the complex interaction of the panels' flexural stiffness, mass, internal damping mechanism and the spatial distribution of the reinforcement. In the present experimental program, twelve one-way slab panels were subjected to the free fall of 10 kg mass from height of 1m to the midspan of the panel. Midspan dynamic displacements and midspan accelerations were measured for each panel. Downward deflections are defined as negative in accordance with the physical direction of loading. The results are presented and discussed individually and comparatively in the sections that follow.

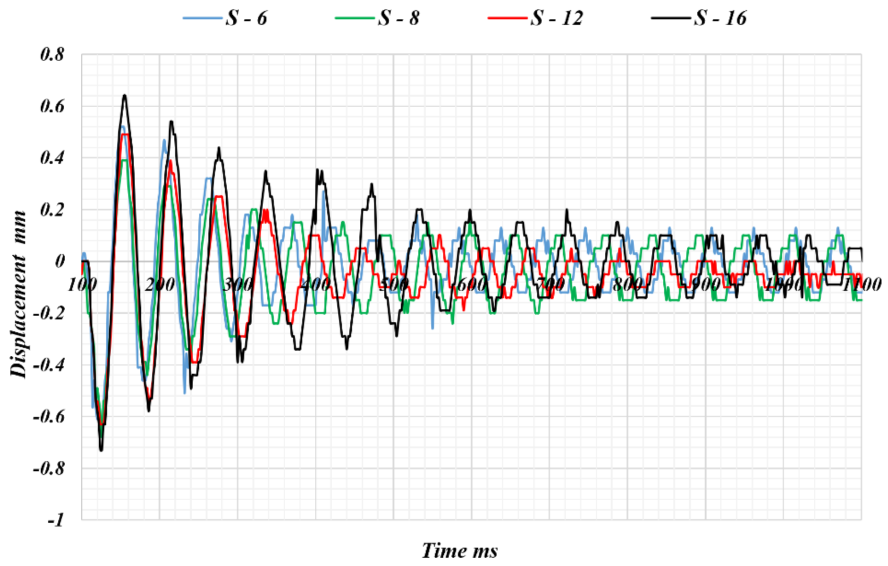

Fig. 5. Midspan displacement for deformed steel specimens. (Upward Disp. +)

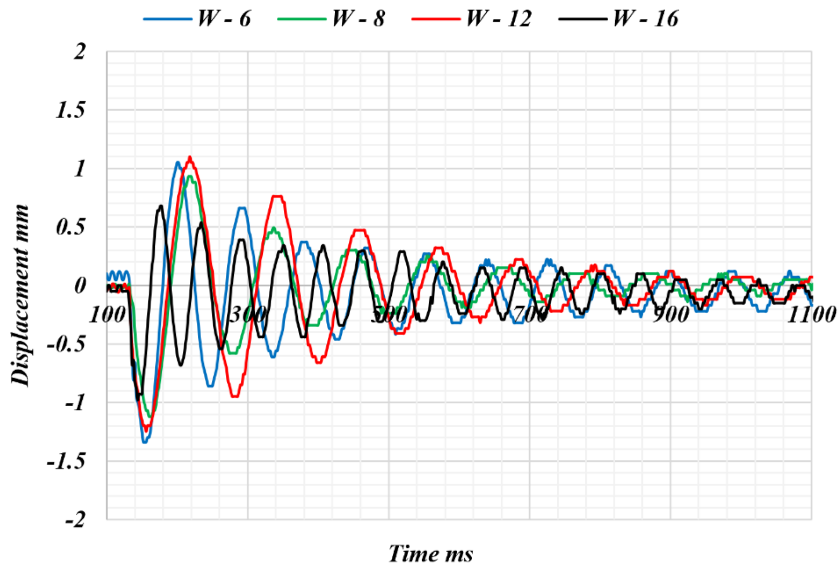

Fig. 6. Midspan displacement for wire rope reinforced panels. (Upward Disp. +)

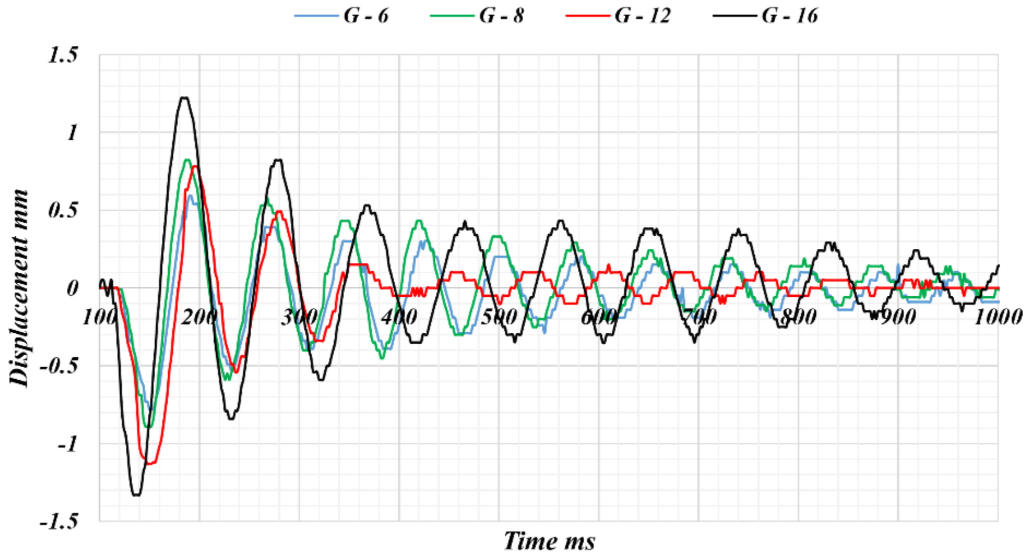

Fig. 7. Midspan displacement for GFRP reinforced panels. (Upward Disp. +)

3.1 Natural Frequency

Since the impact-introduced displacements were of the order of fractions of millimeters - well below any cracking threshold - the section responded in its uncracked elastic state throughout the free-vibration phase, and the governing stiffness is therefore the gross uncracked section stiffness rather than any post-crack effective stiffness. Under these conditions, the natural frequency is primarily controlled by the section geometry, concrete elastic modulus and total mass with reinforcement contributing through its modular ratio effect on the gross transform section stiffness.

Traditional steel reinforced panels exhibited the highest natural frequency values attributed to the high modulus of elasticity of steel reinforcement and the efficient bond between steel bars and the surrounding concrete. Generally, natural frequency decreased with increasing bar diameter due to the increase in the total steel-concrete interfacial contact area resulting to better distribution of bond stresses on reinforcement concrete interfaces.

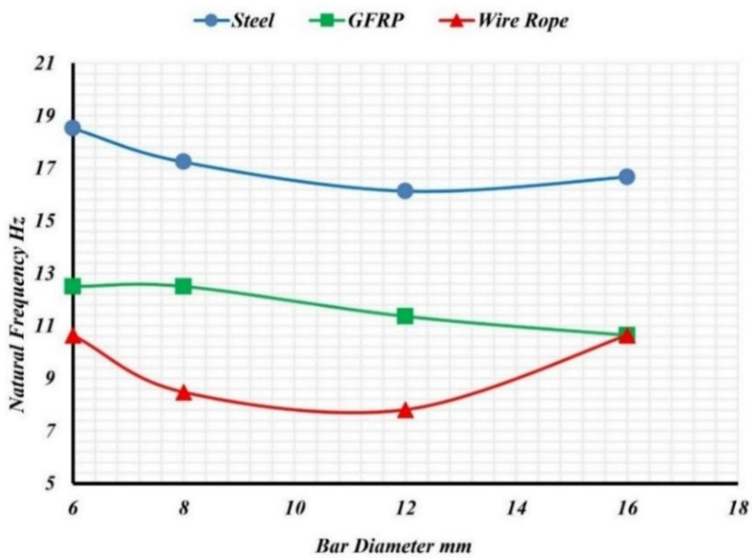

Fig. 8. The effect of bar diameter on natural frequency

In the wire rope reinforced series, the initial decreasing trend from W-6 to W-12 is attributable to the progressive reduction in the number of wire ropes as diameter increases. W-6 contains the greatest number of rope elements, providing more distributed composite interaction with the surrounding concrete and thus a higher cumulative interfacial stiffness contribution. The notably higher frequency of W-16, which departs from the otherwise decreasing trend, warrants careful consideration. A single wire rope of 16mm diameter possesses substantially greater individual flexural rigidity than the smaller diameter ropes used in the other specimens.

The observed trend of decreasing natural frequency with increasing bar diameter in GFRP-reinforced series is physically meaningful and warrants careful interpretation. Since all four panels share identical geometry, concrete grade and reinforcement ratio, the variation in frequency cannot be attributed to differences in mass or gross cross-sectional stiffness. Rather, it reflects the influence of the effective flexural stiffness contributed by the GFRP enforcement itself. Specimens G-6 and G-8 exhibited higher frequencies whereas G-12 and G-16 yielded reduced frequencies. The greater number of bars in G-6 and G-8 distributes the reinforcement more uniformly across the panel width, potentially improving composite action and effective moment of inertia of the transformed section, further supporting the observed frequency values.

A higher natural frequency is preferable as it means that the section is stiffer and this reduces the likelihood of resonance with common dynamic excitation sources (machinery, traffic, people and impact). Slab natural frequency should be well above the dominant excitation frequency to maintain a large frequency separation margin.

3.2 Damping Ratio

The effective viscous damping ratio estimated by the logarithmic decrement method [20] from successive free-vibration peaks ranged from 5.39% for S-6 to 3.04% for S-16, revealing a consistent and monotonically decreasing trend as increasing bar diameter. The inverse relationship between bar diameter and damping ratio in steel reinforced specimens can be attributed to the total steel-concrete interfacial contact area. Specimens reinforced with smaller-diameter bars, possess substantially larger cumulative bond parameter per unit length, generating more extensive micro-frictional interaction at the steel-concrete interface.

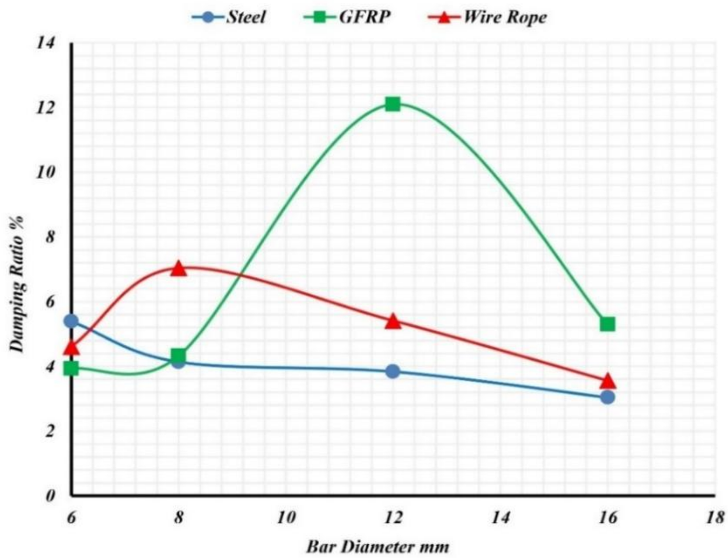

Fig. 9. The effect of bar diameter on damping ratio.

The non-monotonic trend observed across the four specimens reinforced by steel wire ropes is particularly noteworthy. Given that the reinforcement ratio is held constant and the cross-sections remain uncracked, this pattern is unlikely to be governed by crack-induced energy dissipation, which is the dominant mechanism in conventional reinforced concrete. Rather, it may be attributed to the mechanical interaction between the wire rope and the surrounding concrete matrix, whereby the multi-wire helical geometry of the rope introduces frictional inter-wire slip at the strand level. The lowest damping ratio is recorded for W-16 (ζ = 3.56%). The three 16 mm wire ropes provide a limited total steel-concrete interface parameter. Consequently, the panel oscillates with low damping and sustains amplitude - a response pattern consistent with the behavior of near elastic, lightly damped structural members.

The notably elevated damping ratio of specimen G-12 is a physically significant observation that warrants careful consideration. Given that the enforcement ratio is held constant across all the specimens and the sections remain uncracked, this anomaly cannot be attributed to crack-induced energy dissipation. Rather, it's more appropriately interpreted in terms of the relatively lower elastic modulus of the 12 mm GFRP bars combined with the reduced bar count, which together yield a more flexible reinforcement arrangement.

Panels reinforced by large-diameter GFRP bars consistently exhibited higher damping ratio than their steel bar and wire rope counterparts, meaning that the use of coarse configuration of GFRP reinforcement is preferable in cases where high damping is required. Despite the high cost of GFRP reinforcement, it's beneficial to be used in structural elements exposed to dynamic vibrations and severe corrosive environment like bridge decks and girders.

A high damping ratio means that the slab dissipates dynamic energy more rapidly, causing vibrations to decay faster after excitation ceases. Higher damping reduces dynamic amplification and limits peak displacement, and stress under dynamic loading. Additionally, higher damping improves serviceability and fatigue performance due to the reduction in sustained dynamic stresses.

3.3 Dynamic Amplitude

The larger amplitude of S-16 compared to other steel reinforced specimens is attributable to the concentration of bending stiffness into only three bars, which simultaneously reduces the total steel concrete interface parameter, allowing a greater fraction of the impacted kinetic energy to be converted into elastic strain energy and peak displacement. The relatively modest amplitude of S-12, despite its intermediate diameter, reflects the beneficial interaction between its five-bar configuration and the concentrated bond stress intensity per bar. The narrowness of the amplitude range across the series (0.62-0.75 mm) compared to GFRP series (0.78-1.33 mm), reflects the uniformly high elastic moduli of the steel bars relative to the more variable and generally lower GFRP moduli.

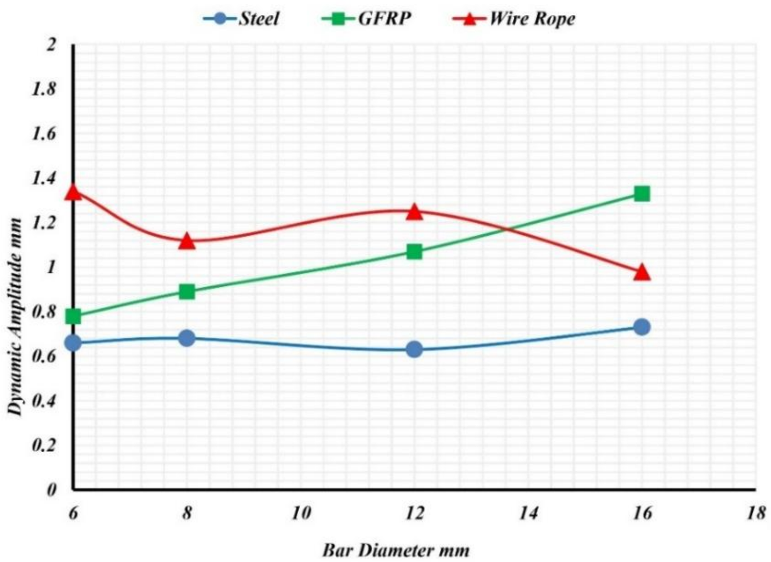

Fig. 10. The effect of bar diameter on dynamic amplitude

Except for the slight reversal between W-8 and W-12, the general trend is one of decreasing peak displacement with increasing wire rope diameter, which is physically consistent with the expected dynamic stiffness behavior of uncracked composite sections. The number of wire ropes decreases substantially from W-6 to W-16, progressively reducing the total steel-concrete interfacial contact area and, consequently, the distributed composite action across the slab width. Specimen W-6 benefits from the most extensive interfacial engagement which enhances the effective flexural rigidity of the section and thereby limits the peak displacement response to the dynamic impulse. The slight departure from the monotonic trend at W-12, which registers a higher peak displacement than W-8, may be attributed to the competing influence of the individual rope flexural rigidity.

G-16 records the largest initial dynamic amplitude in the series, while G-6 records the smallest. This monotonic increase with bar diameter follows the same physical mechanism as observed in the steel series: as bar diameter increases, the total GFRP concrete interface parameter decreases progressively. The reduction in total interface parameter allows a greater fraction of the imparted kinetic energy to be converted into elastic strain energy and manifest as peak midspan displacement. The lower dynamic amplitude is preferred as it refers to the smaller displacements and stresses under dynamic loading protecting structural integrity and occupant comfort. Excessive dynamic amplitude causes human discomfort, equipment malfunction and potential fatigue cracking in the slab.

Table 6. Summary of test results

Reinforcement	Damping ratio %	Natural frequency Hz	Dynamic amplitude mm
S-6	5.39	18.52	0.66
S-8	4.14	17.24	0.68
S-12	3.84	16.13	0.63
S-16	3.039	16.67	0.73
W-6	4.611	10.64	1.34
W-8	7.04	8.47	1.12
W-12	5.414	7.8	1.25
W-16	3.56	10.64	0.98
G-6	3.934	12.5	0.78
G-8	4.323	12.5	0.89
G-12	12.1	11.36	1.07
G-16	5.3	10.64	1.33

3.4 Midspan Acceleration

Upon impact, all steel reinforced panels displayed an initial sharp acceleration peak, followed by a free-vibration decay phase whose rate varied considerably among the tested configurations. S-6 recorded the highest initial positive acceleration peak with relatively rapid attenuation reflecting a higher damping. This behavior suggests that the more distributed reinforcement arrangement associated with smaller diameter bars promotes greater energy dissipation other reinforcement concrete interface, resulting in a higher effective damping ratio. Midspan acceleration data in Figure 12 indicate that, within the deformed steel bar series, the viscous damping ratio decreases as bar diameter increases. This trend is physically consistent with the reduction in the number of reinforced reinforcing bars and the corresponding decrease in total reinforcement-concrete interfacial area as bar diameter decreases, which in turn limits the frictional and bond-related energy dissipation mechanisms that governs the damping response under low energy impact loading.

The non-monotonic relationship between bar diameter and damping ratio observed in the GFRP series - where G-12 outperforms both smaller and larger diameter configurations - suggests that the energy dissipation mechanism in GFRP reinforced panels is governed by a complex interaction of factors rather than bar diameter alone. At intermediate diameters such as 12 mm, the adhesion characteristics between the GFRP bar and the concrete matrix and the local confinement effect of the surrounding concrete produce a more favorable condition for interfacial energy dissipation. In contrast, the finer reinforcement distribution of G-6 and G-8, while providing greater contact area, appears to generate a stiffer post impact response, whereas the larger G-16 bars tend to concentrate damage without a proportional increase in distributed energy dissipation.

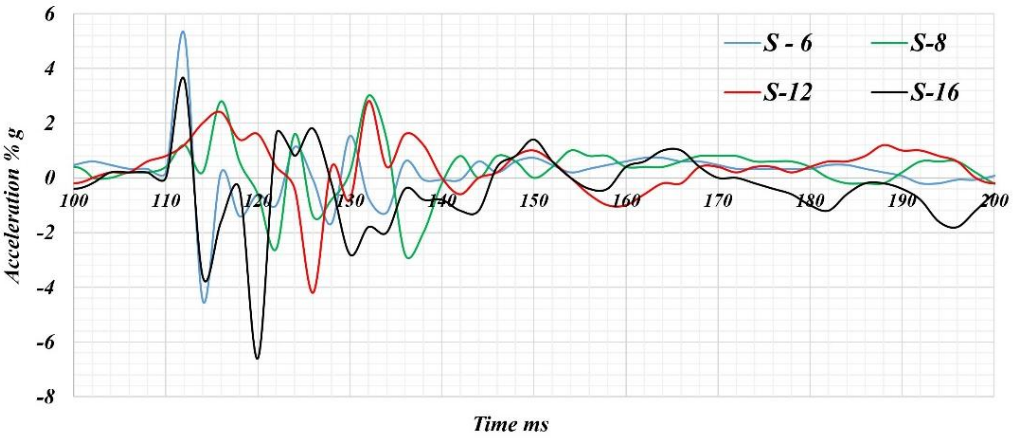

Fig. 11. Midspan acceleration for deformed steel specimens

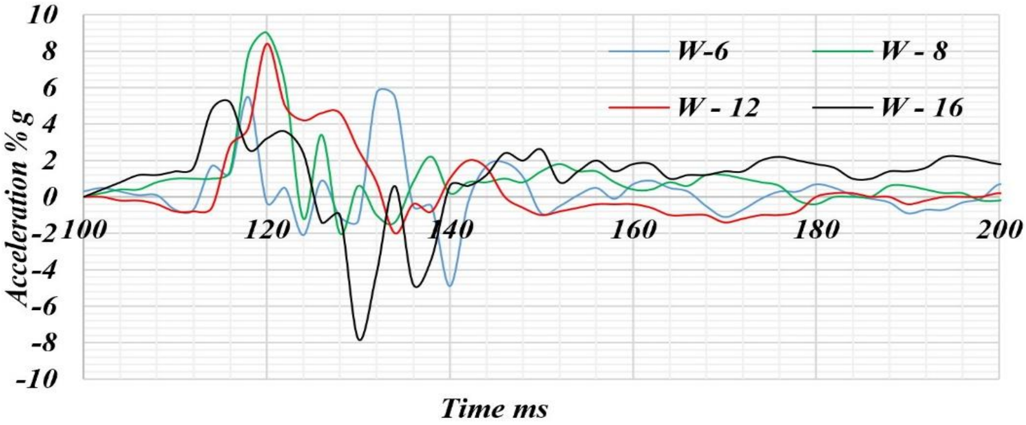

Fig. 12. Midspan acceleration for wire rope reinforced panels.

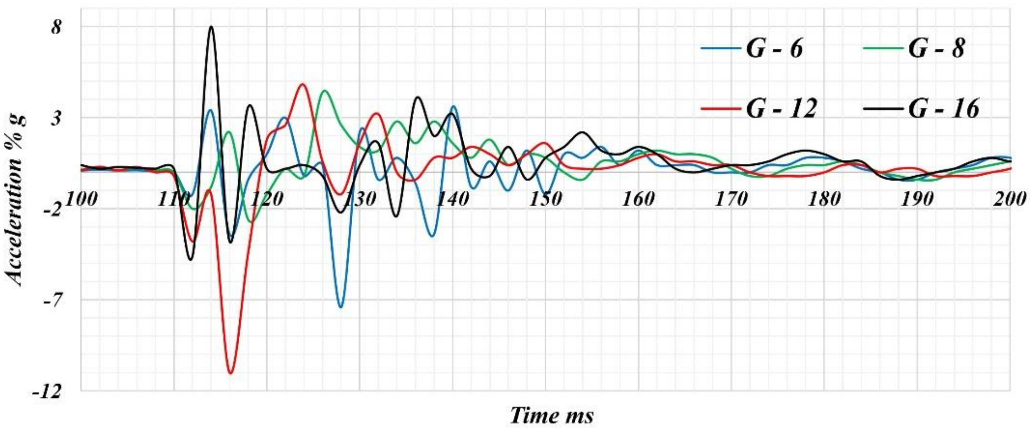

Fig. 13. Midspan acceleration for GFRP reinforced panels.

The observation that W-8 outperforms W-6 in terms of energy dissipation, despite having larger bar diameter, indicates that the relationship between wire rope diameter and damping capacity is not strictly monotonic within this series. This behavior may be partly attributed to the diameter-dependent variation in internal wire-to-wire friction within the rope strands.

Overall, the midspan acceleration data showed the same behavior of the three series in terms of damping ratio calculated from the midspan displacement graphs. In deformed steel reinforced panels, the damping ratio decreases when increasing bar diameter. in wire rope reinforced specimens, G-8 exhibited the faster acceleration diminishing, and in GFRP reinforced panels, G-12 showed relatively rapid acceleration wave excitation.

3.5 Feasibility and Applicability Analysis

The practical applicability of the three reinforcement types investigated in this study varies considerably in terms of cost, workability, anchoring, bond characteristics and durability. Deformed steel bars remained the most established and cost-effective reinforcement option, benefiting from standardized production, widely available skilled labor, and well-developed design codes. However, their susceptibility to corrosion in aggressive environments - particularly in chloride-rich or carbonated concrete - represents a long-term durability concern that may lead to significant maintenance and repair costs over the service life of the structure.

GFRP bars offer a compelling alternative in corrosive environments due to their inherent resistance to electrochemical corrosion, significantly reducing long-term maintenance costs. Their high tensile strength to weight ratio also facilitates handling and placement. However, the initial material cost of GFRP bars is considerably higher than that of conventional steel. Additionally, GFRP bars exhibit linear elastic behavior with no yielding plateau. Cutting and bending GFRP bars onsite also require specialized tools, adding to labor complexity.

Steel wire rope presents a fundamentally different set of practical challenges. While it offers flexibility and high tensile capacity, it's use as conquering reinforcement introduces several significant workability concerns. The absence of standardized anchoring system for wire rope embedded in concrete creates difficulties in ensuring adequate force transfer at the end of structural elements, potentially leading to premature anchorage failure. The helical geometry of wire rope results in a lower effective modulus of elasticity compared to solid steel bars and its smooth surface finishes produces inferior bond characteristics with the surrounding concrete matrix. Furthermore, wire rope is susceptible to internal corrosion between individual wires, which is difficult to detect and may progress unnoticed within the concrete section, posing a long-term durability risk comparable to or exceeding that of conventional steel in aggressive environments. The higher labor costs associated with cutting, positioning and securing wire rope within formwork, combined with the lack of established design provisions, father limits its immediate applicability as a primary reinforcement system.

4. Conclusions

Depending on the results of the tests performed on the twelve specimens included in the experimental program, it is important to summarize the main conclusions as follows:

- Natural frequency followed the ranking deformed steel > GFRP > wire rope. The highest natural frequency was recorded by S-6 and most of the natural frequency values decreased when increasing reinforcement diameter.
- Specimens reinforced with the large-diameter bars produced sharp, high amplitude impact spikes and pronounced rebound pulses. In contrast, reducing reinforcement bar diameter results in lower peak amplitudes but more sustained pulse durations.
- In deformed steel reinforced panels, the viscous damping ratio decreased when increasing reinforcement diameter, demonstrating that panels with finer reinforcement distributions achieve significantly higher damping. While in steel wire rope reinforced panels the damping ratio was higher in specimens reinforced by large bar diameter.
- In GFRP series, however, the damping ratio did not follow a consistent linear trend with bar diameter. G-12 exhibited the highest stamping ratio, exceeding both the G-6 and G-16 specimens. This anomalous behavior is attributed to the interplay of several physical mechanisms specific to GFRP bars. At intermediate diameters, greater frictional energy dissipation is generated; the adhesion characteristics between the GFRP bar surface and the surrounding concrete matrix are diameter-dependent, with the G-12 bar producing an optimal bond condition.
- Distributed fine-bar configurations should be preferred over concentrated large-bar configurations, even when both provide equivalent static strength as finer reinforcement distributions provide substantially greater total interface parameter at an equivalent reinforcement area, thereby producing higher system-level damping.

- GFRP reinforced panels consistently exhibited higher damping ratio than their steel and wire-reinforced panels in the coarse reinforcement configuration (12 and 16 mm reinforcement bars). Specimen G-12 achieved the most rapid extinction outperforming both the stiffer 16 mm configuration and the more flexible 6 mm configuration.
- Natural frequency of wire rope-reinforced panels is the lowest in the three series. However; the effect of bar diameter on natural frequency is almost identical between steel and wire- reinforced specimens.
- Midspan acceleration showed agreement with displacement readings in terms of vibration damping in all the three series.

It is recommended to extend the study in the future by using more reinforcement systems (i.g. hybrid reinforcement system) and different dynamic impacts (i.g. high velocity impact). The effect of changing concrete mixture also could be studied in future. Additionally, it is recommended to apply theoretical analysis of the dynamic response if slab panels are reinforced by steel and alternatives.

References

[1] Firmo JP, Fibre-Reinforced Polymer Reinforcement Towards More Durable and Sustainable Concrete Structures. In: Janberg N, editor. Sustainability in Structural Concrete Design. Zurich: International Association for Bridge and Structural Engineering; 2024. p. 320-360. https://doi.org/10.2749/sed020.ch14

[2] Ruiz Emparanza A, Durability assessment of GFRP rebars in marine environments. Constr Build Mater. 2022;329:127028. https://doi.org/10.1016/j.conbuildmat.2022.127028

[3] Ahmed E, Design of Bridge Deck Slabs Using Glass Fiber-Reinforced Polymer (GFRP) Bars of Different Grades. In: The 9th International Conference on Short and Medium Span Bridges. Calgary: SMSB; 2014. p. 1-10.

[4] Carvelli V, Fatigue behaviour of concrete bridge deck slabs reinforced with GFRP bars. Compos Part B Eng. 2010;41:560-567. https://doi.org/10.1016/j.compositesb.2010.06.006

[5] Liu T, Experimental Research on Damping and Bonding Properties of Concrete Reinforced with GFRP Bars. In: 12th Biennial International Conference on Engineering, Construction, and Operations in Challenging Environments. Honolulu: American Society of Civil Engineers; 2010. p. 2793-2805. https://doi.org/10.1061/41096(366)264

[6] Sadraie H, Dynamic performance of concrete slabs reinforced with steel and GFRP bars under impact loading. Eng Struct. 2019;62-81. https://doi.org/10.1016/j.engstruct.2019.04.038

[7] Mousavi T, Impact response of hybrid FRP-steel reinforced concrete slabs. Structures. 2019;436-448. https://doi.org/10.1016/j.istruc.2019.02.013

[8] Salih YA, Impact Resistance of GFRP Reinforced Concrete One-Way Slabs. Inf Sci Lett. 2022;1267-1275. https://doi.org/10.18576/isl/110426

[9] Anas SM, Ultra-high-performance concrete and C-FRP tension Re-bars: A unique combination of materials for slabs subjected to low-velocity drop impact loading. Front Mater. 2022;1061297. https://doi.org/10.3389/fmats.2022.1061297

[10] Dong S, Dynamic impact behaviors and constitutive model of super-fine stainless wire reinforced reactive powder concrete. Constr Build Mater. 2018;602-616. https://doi.org/10.1016/j.conbuildmat.2018.07.027

[11] Wu Q, Blast-resistance characteristics and design of steel wire reinforced ultra-high performance concrete slabs. Int J Impact Eng. 2024;105059. https://doi.org/10.1016/j.ijimpeng.2024.105059

[12] Wu Q, Blast and impact resistance of stainless steel wire-reinforced ultra-high performance concrete door panels: Numerical analyses and design insights. Thin-Walled Struct. 2025;113485. https://doi.org/10.1016/j.tws.2025.113485

[13] American Concrete Institute. Building Code Requirement for Structural Concrete (ACI 318-19). Farmington Hills: American Concrete Institute; 2019.

[14] Abdulsahib WS, Low Velocity Impact Response of Reinforced Concrete Flat Slabs. Open Civ Eng J. 2023;17:E230113. https://doi.org/10.2174/18741495-v17-e230113-2022-75

[15] Anas SM, Influence of Supports on the Low-Velocity Impact Response of Square RC Slab of Standard Concrete and Ultra-High Performance Concrete: FEM-Based Computational Analysis. Buildings. 2023;13051220. https://doi.org/10.3390/buildings13051220

[16] ASTM International. ASTM C39/C39M-21: Standard test method for compressive strength of cylindrical concrete specimens. West Conshohocken: ASTM International; 2021.

[17] International Organization for Standardization. ISO 10406-1: Fibre-reinforced polymer (FRP) reinforcement of concrete - Test methods. Geneva: ISO; 2025.
[18] ASTM International. ASTM A615/A615M-18: Standard Specification for Deformed and Plain Carbon-Steel Bars for Concrete Reinforcement. West Conshohocken: ASTM International; 2018.
[19] ASTM International. ASTM A931/A931M-18: Standard test method for tension testing of wire rope and strand. West Conshohocken: ASTM International; 2018.
[20] Chopra AK. Dynamics of Structures: Theory and Applications to Earthquake Engineering. Pearson Education; 2017.